

## Catalytic combustion of toluene over electrochemically promoted Ag catalyst

Ning Li, François Gaillard\*

*Institut de recherches sur la catalyse et l'environnement de Lyon (IRCELYON), UMR 5256 CNRS - Université de Lyon, 2 avenue Albert Einstein, F-69626 Villeurbanne cedex, France*

### ARTICLE INFO

*Article history:*

Received 9 June 2008

Received in revised form 10 September 2008

Accepted 13 September 2008

Available online 25 September 2008

*Keywords:*

Electrochemical promotion of catalysis

EPOC

Toluene combustion

VOC

Ag

Impregnation

### ABSTRACT

Evident electrochemical promotion of the complete catalytic oxidation of toluene in the temperature range 300–330 °C was observed, for the first time, on a silver film catalyst prepared by direct impregnation onto a Y<sub>2</sub>O<sub>3</sub> stabilized ZrO<sub>2</sub> (YSZ) solid electrolyte. It was found that the toluene conversion into CO<sub>2</sub> and H<sub>2</sub>O on such a catalyst can be significantly promoted upon cathodic polarization, i.e. oxygen removal from the catalyst surface. The promotion effect increases with the temperature within the investigated range. Furthermore, it was found that the promotion effect was also strongly influenced by toluene and oxygen concentrations. With increasing the toluene concentration, the rate enhancement decreased while the Faradaic efficiency shows a volcano type behaviour. The relationships between the rate enhancement and Faradaic efficiency with the oxygen concentration are on the contrary, i.e. there is an optimum for rate enhancement when oxygen concentration is about 2%, the Faradaic efficiency monotonically decreasing with oxygen concentration. Finally, the promotion effect also increased with the thickness of Ag film, which may be interpreted by more available active sites.

© 2008 Elsevier B.V. All rights reserved.

### 1. Introduction

From the beginning of the 21st century, due to increasing social and political concern in environment, the removal of volatile organic compounds (VOCs) emitted from industrial and domestic processes has drawn a lot of attention. A cheap and efficient way of VOCs removing is their complete catalytic oxidation to harmless products such as H<sub>2</sub>O and CO<sub>2</sub> [1–6]. Supported Pt and Pd are well established as efficient catalysts for VOCs combustion [1–3]. However, due to the high cost and limited reserve of such noble metals, the quest for cheaper and more environmentally friendly catalytic materials are of an ever-increasing importance for tomorrow's applications.

In 1981, Stoukides and Vayenas [7] have shown the ability of electrochemistry to modify the rate and the selectivity of the catalytic ethylene oxidation on silver. This process, called non-Faradaic electrochemical modification of catalytic activity (NEMCA) or more recently electrochemical promotion of catalysis (EPOC) has drawn much attention in the past two decades, due to its remarkable versatility and possible application to many catalytic systems [8–20]. EPOC is based on the control of the catalyst work function by applying a small potential or current to a catalyst/electrode interfaced to a solid electrolyte. During the past

years, most of the work on EPOC for hydrocarbon combustion focused on lower molecular weight alkanes or alkenes, such as methane, ethylene, propane, propylene, etc. [10–14]. However, for environment protection purpose, the removal of aromatic organic compounds is still much more important, because they can be more toxic and harmful.

To our knowledge, the work dealing with the application of EPOC to the removal of aromatic organic compounds is very scarce. The pioneering study of EPOC applied to toluene combustion was carried out using RuO<sub>2</sub>/YSZ [16], operated at temperatures from 400 to 500 °C. Promotional effects were found for both anodic (1.5 V) and cathodic (-1.5 V) polarizations, enhancing the rate of toluene oxidation by factors of 8 and 4, respectively. These promotional effects were non-Faradaic. These results clearly demonstrated that EPOC could be used in this field. Nevertheless, to fulfill the needs encountered in real application, some more active catalysts (efficient at lower temperatures) are still to be found. One possible route was the use of catalytically active oxides such as perovskites, able to act as a catalyst-electrode, but previous results have shown that EPOC effect is quite limited [11].

Therefore, in a recent work [21], we explored for the first time the EPOC performance of an Ag film catalyst deposited on YSZ for the total oxidation of toluene, and found a significant NEMCA effect when applying negative potential or current at a temperature much lower (300 °C) but still compatible with a sufficient oxygen ions conductivity of YSZ. However, these results were obtained

\* Corresponding author. Tel.: +33 4 7244 8066; fax: +33 4 7244 5399.  
E-mail address: [francois.gaillard@ircelyon.univ-lyon1.fr](mailto:francois.gaillard@ircelyon.univ-lyon1.fr) (F. Gaillard).

using an Ag paint as the catalyst thin film precursor, as it is usual in works dealing with EPOC [22,23], but such a method also suffers from some drawbacks:

1. The composition of the commercial Ag paste is usually unknown, some organic additives or impurities may also lead to catalyst poisoning.
2. To make sure the surface is clean and to exclude the interference of organic residue, the metallic films prepared by this method need to be pretreated at high temperatures (above 500 °C) in pure oxygen or air for the decomposition of the organic compounds. In the specific case of Ag, such a high temperature treatment would lead to a loss of metal by reactive thermal evaporation of the silver oxide (AgO) in a background of molecular oxygen [24].

From a practical point of view, it is necessary to find a simple, efficient and cost-effective way to prepare such catalytic films. The thermal decomposition of RuCl<sub>3</sub> precursor [16] to obtain RuO<sub>2</sub> deposits on YSZ is a good example of such a simple and efficient method.

Wet impregnation is a method, which is widely used for the preparation of industrial supported noble metal catalysts. Recently, Dorado et al. [25–29] reported that Pt, prepared by a wet impregnation method onto Na (or K)-β-Al<sub>2</sub>O<sub>3</sub> solid electrolyte, can be electrochemically promoted for several reactions, such as the selective catalytic reduction of nitrogen oxides by propylene [25–27], the catalytic combustion of propylene [28] and the oxidation of CO [29]. In light of these works, we carried out for the first time the investigation of Ag films deposited on YSZ by wet impregnation from AgNO<sub>3</sub> aqueous solution followed by a reduction step with H<sub>2</sub>. These systems were evaluated under electrochemical promotion of complete catalytic oxidation of toluene. To get a deep insight into the EPOC performance of the Ag film catalyst, the effect of several parameters such as reaction temperature, toluene and oxygen concentrations, and Ag film thickness were also investigated.

## 2. Experimental

### 2.1. Catalyst preparation

The electrochemical catalyst consisted of a thin Ag film (working electrode (WE), geometric area of c.a. 1.8 cm<sup>2</sup>) deposited on the one side of a 17 mm in diameter and 1 mm thick Y<sub>2</sub>O<sub>3</sub> stabilized ZrO<sub>2</sub> electrolyte disk (YSZ, 8 mol% Y<sub>2</sub>O<sub>3</sub>), with gold counter and reference electrodes on the other side.

As the first step, the gold counter and reference electrodes were deposited on the one side of the YSZ disk, according to the method described in the literature [21,30,31] via deposition of a thin layer of A1644 gold paint (METALOR, France), followed by firing at 800 °C in oxygen flow for 2 h (heating ramp was 2 °C min<sup>-1</sup>). Subsequently, the Ag film was deposited on the other side of YSZ pellet by the direct impregnation of AgNO<sub>3</sub> aqueous solution. The disk was then dried at room temperature, then reduced in H<sub>2</sub> at 300 °C for 2 h (heating ramp: 2 °C min<sup>-1</sup>) in a quartz reactor and then cooled down to room temperature. After that, the complete system was checked for electrodes electronic conductivity at room temperature and assembly ionic conductivity at 300 °C. To investigate the influence of working electrode thickness, electrochemical catalysts were prepared in the same way but using different volumes of AgNO<sub>3</sub> solution. The thickness of the Ag film was estimated from the weight increase of the pellet after impregnation and reduction and from the geometric surface area

of working electrode, assuming the density of metallic Ag. For the remaining of the study, two samples were selected, with estimated Ag film thickness being 1.8 and 3.9 μm, considering 10.5 kg L<sup>-1</sup> for Ag density [32] and 1.8 cm<sup>2</sup> for the geometric area of Ag film.

### 2.2. Characterization techniques

#### 2.2.1. XRD

XRD patterns of the pellet samples were obtained on a Bruker D8 Advance, using the Cu Kα line (0.15418 nm). The angular scan was performed from 10° to 70° (2θ), with 0.02° steps. The average crystallite size was estimated using the Scherrer equation:

$$D = \frac{0.90\lambda}{\beta \cos \theta} \quad (1)$$

where  $D$  is the average crystallite size (nm),  $\lambda$  the incident wavelength (nm),  $\beta$  the corrected full width at half maximum (radian) and  $\theta$  the Bragg angle.

#### 2.2.2. SEM

The Ag/YSZ samples were investigated by SEM and EPMA using a Jeol JSM-5800LV scanning electron microscope, operated at 20 kV and 75 μA and controlled by SPIRIT (Princeton Gamma Tech) software.

### 2.3. Catalytic tests

The catalytic reaction was carried out using a specific electrochemical quartz reactor as described elsewhere [30] under atmospheric pressure. For a typical activity evaluation, a mixture of O<sub>2</sub>, toluene and He (1% O<sub>2</sub>, 500 ppm toluene, He as the balance, total flow rate, 100 mL min<sup>-1</sup>) was fed over the Ag catalyst. The reactants and products were analyzed by a PerkinElmer Clarus 500 gas chromatograph with a TCD detector. As the major product of the reaction, the yield of CO<sub>2</sub> was used to evaluate the toluene conversion.

A Voltalab® system (Radiometer Analytical PGP 201) was used for constant current or potential application, i.e. for galvanostatic or potentiostatic operation. Before applying any potential or current, the catalysts were submitted to a standardization procedure, consisting in overnight pretreatment under the reaction conditions.

Two classical parameters were used to describe the magnitude of electrochemical promotion:

1. The apparent Faradaic efficiency,  $\Lambda$ , defined from:

$$\Lambda = \frac{r - r_0}{I/nF} = \frac{\Delta r}{I/nF} \quad (2)$$

where  $r_0$ , in mol O/s (case of an O<sup>2-</sup> conductor), is the catalytic rate at OCV;  $r$  is the catalytic rate under polarization;  $n$  is the number of exchanged electrons during the electrode reaction ( $n = 2$  with an O<sup>2-</sup> conductor) and  $\Delta r$  is the catalytic reaction rate change associated with the current  $I$ . A catalytic reaction exhibits the NEMCA effect when  $|\Lambda| > 1$ . A reaction, which is accelerated by a negative current or overpotential (oxygen removed from the catalyst surface in the present case) with a value of  $\Lambda$  lower than -1 exhibits an electrophilic NEMCA behaviour. Conversely, when the catalytic reaction is promoted by a positive current or overpotential (here oxygen supplied to the catalyst surface) with  $\Lambda > 1$ , its NEMCA behaviour is called electrophobic.

2. The rate enhancement,  $\rho$ , defined from:

$$\rho = \frac{r}{r_0} \quad (3)$$

where  $r$  is the electro-promoted catalytic rate and  $r_0$  is the unpromoted (open-circuit) catalytic rate.

### 3. Results and discussion

#### 3.1. Characterizations

##### 3.1.1. XRD

The XRD profiles for the two samples as prepared are shown on Fig. 1. It is clear that silver species are only observed as metallic Ag and that no peak of silver oxide or nitrate can be detected, which means that precursor decomposition and reduction are complete. The ratio between the intensity of the peaks related to Ag and YSZ increased with the thickness of Ag film. According to the Scherrer equation, the average size of Ag crystallites was estimated about 100 nm for both samples, which means that, under the same preparation conditions, the Ag amount has no evident effect on the average particle size. Moreover, from this average size, the

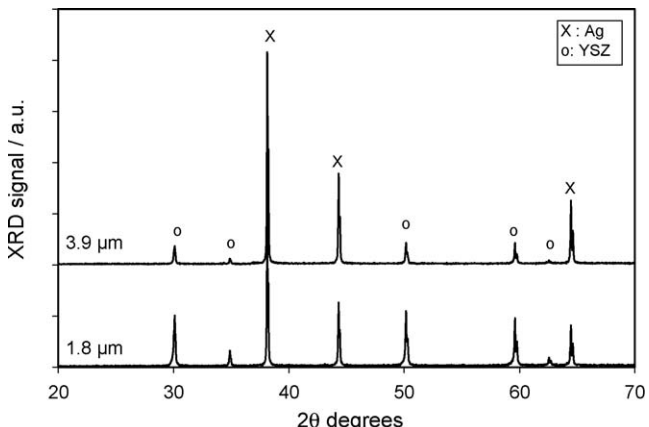


**Fig. 1.** XRD profiles of the Ag catalysts with different thicknesses: Ag film thickness: 1.8  $\mu\text{m}$  (lower trace); 3.9  $\mu\text{m}$  (upper trace).

dispersion of Ag on the two samples was estimated around 1%. This value of dispersion is a bit higher than those typically obtained by application of metal paints (0.5%) [28,33], but far lower than those reported in the case of sputtered films (15–50%) [34,35].

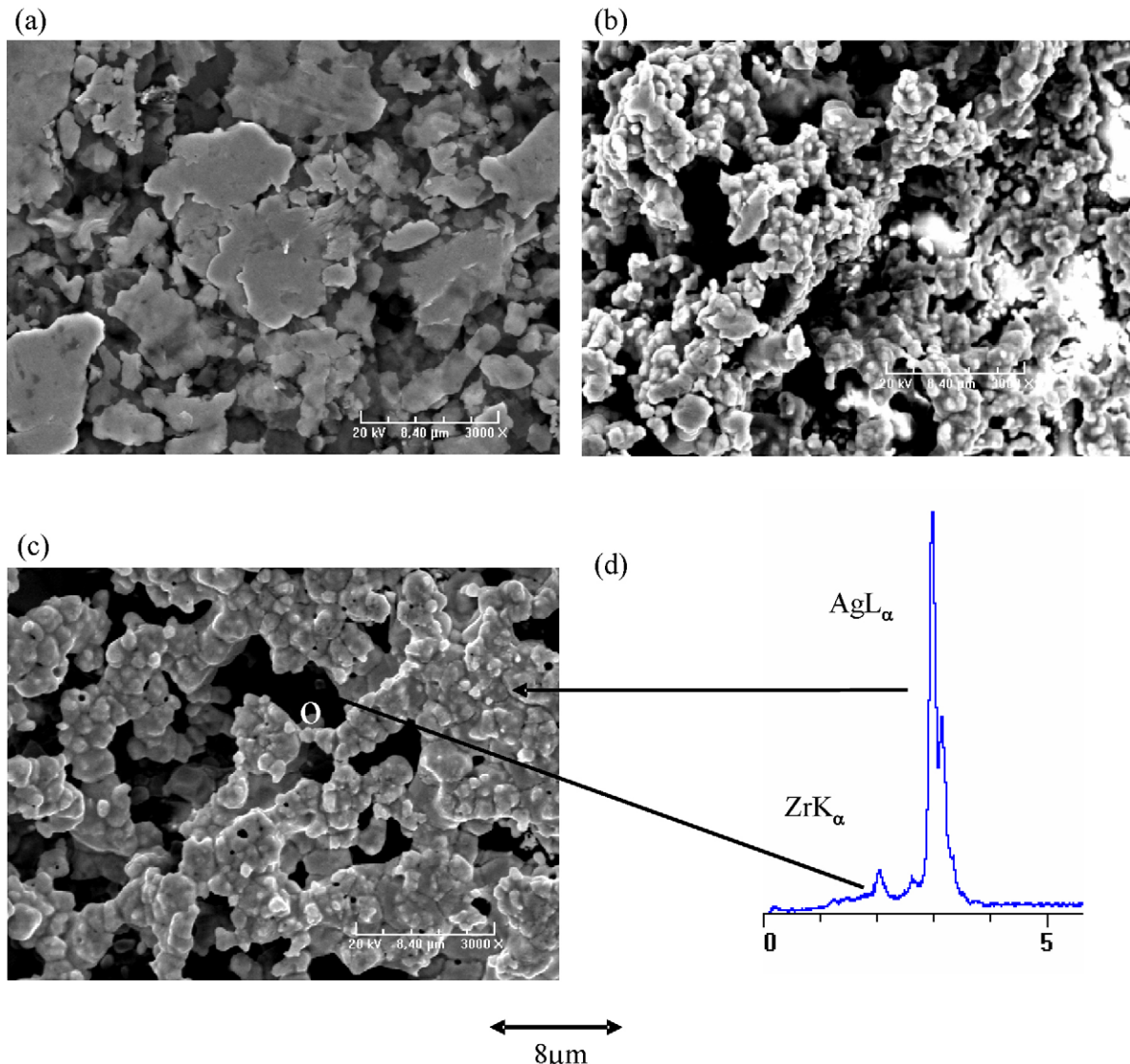


**Fig. 2.** SEM micrographs of the Ag catalyst films: Ag paint (a), Ag film obtained by impregnation 1.8  $\mu\text{m}$  thick (b) and 3.9  $\mu\text{m}$  thick (c), EPMA spectrum (d).

### 3.1.2. SEM

For comparison purpose, Fig. 2(a) is relative to the SEM micrograph of a silver paint commonly used in similar studies [36,37]. Massive and flat-top silver blocks can be observed for such deposits. Conversely, Fig. 2(b) and (c) are relative to silver films obtained by the wet impregnation/H<sub>2</sub> reduction procedure and they exhibit a very porous texture formed by small agglomerated grains. This is consistent with a much lower particle size as estimated by XRD (100 nm) compared to 1000 nm often reported in the literature for deposits obtained by paints [33]. The thicker film (c) does not exhibit a marked change in topography, but larger grains and flat tables are favored, especially near the rim of the film, exhibiting a more massive topography. EPMA analysis (d) clearly shows that surface coverage is not complete, as proved by the Zr K $\alpha$  signal originating from the dark looking zones of SEM micrographs. X-ray mapping of Ag L $\alpha$  and Zr K $\alpha$  exactly matches the clear and dark zones of SEM micrographs, respectively. Quantitative analysis corresponding to the zone depicted in Fig. 2(c) indicates about 85 at.% Ag and 15 at.% Zr (Y from YSZ cannot be analyzed unambiguously here). Such a discontinuous structure is likely to favor the formation of tpb between YSZ, porous Ag layer and reactants. Moreover, the porous texture should much improve Ag–reactant contact.

### 3.2. Catalytic performances

As a preliminary work, we investigated the activity of the YSZ pellet only coated with gold counter and reference electrodes on its back side (blank experiment). It was found that the activity of the YSZ substrate for the toluene combustion is very low. Neither CO<sub>2</sub> peak nor detectable toluene conversion can be observed at temperatures up to 350 °C, which means that we can safely attribute any further conversion of toluene below this temperature to the activity of Ag film catalyst.

#### 3.2.1. Catalytic activity of Ag film under open circuit, -1 V and -2 $\mu$ A at 330 °C

As shown in Fig. 3a, the Ag film catalyst (thickness: 1.8  $\mu$ m) deposited on YSZ was found to be active for toluene combustion. Evident CO<sub>2</sub> yield (about 5%) could be achieved even at such a relatively low temperature (330 °C) and high space velocity (accordingly to the volume of the active phase, the 100 mL min<sup>-1</sup> flow corresponds to a GHSV of  $1.85 \times 10^7$  h<sup>-1</sup>). The open circuit voltage (OCV) was measured as -110 mV with respect to Au reference electrode.

After applying a negative external potential (-1 V), the toluene conversion on Ag catalyst was improved significantly. Over it, the yield of CO<sub>2</sub> increased rapidly up to 21% (about 3.5 times its initial value) and then reached a plateau after some minutes. According to the low current values (about -2  $\mu$ A after stabilization), this duration is very compatible with the building of a continuous oxygen ion monolayer at the surface of an electrode of such dimension. From the current measured at stable conversion, the calculated Faradaic efficiency  $\Lambda$  was -8200, which means that the promotion is highly non-Faradaic, i.e. a strong NEMCA effect is observed. It is worth mentioning that such a Faradaic efficiency (-8200) is comparable with the value reported for paste-made Ag catalyst ( $\Lambda$  ranging from -2100 to -39,700) [21]. The activity recovers very quickly its initial value upon turning the potential off, as previously observed with the paste-made Ag catalyst. This experiment can be totally repeated and similar results can be obtained when the potential is turned on again, indicating that it is a repeatable, reversible and non-permanent effect.

Likewise, from Fig. 3b, we can see that an evident improvement can also be realized by applying a very low negative current

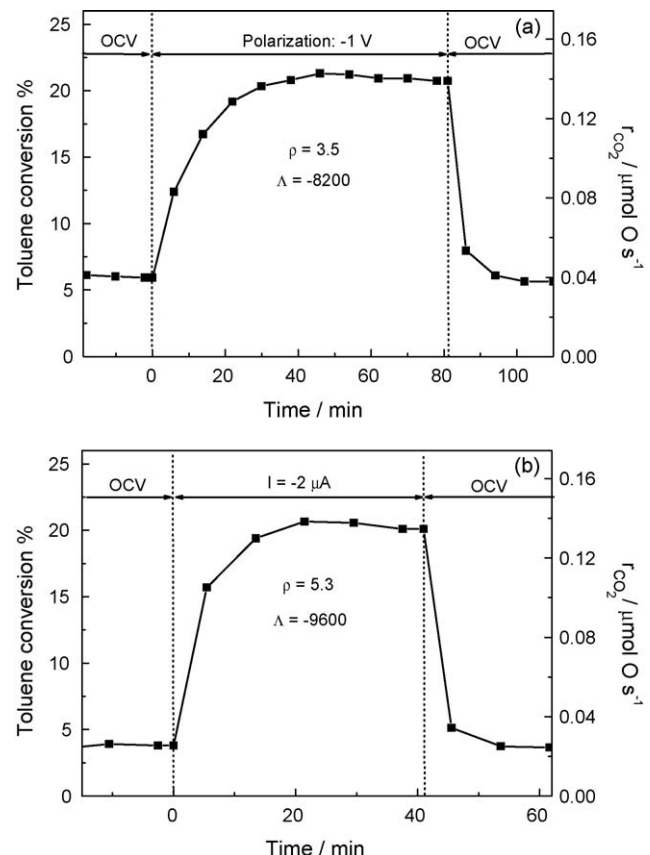


Fig. 3. Effect of -1 V (a) and -2  $\mu$ A (b) on the activity of Ag film catalyst (thickness: 1.8  $\mu$ m) deposited on YSZ pellet. Reaction condition: 1% O<sub>2</sub>, 500 ppm toluene, He balance; total flow rate, 100 mL min<sup>-1</sup>, 330 °C.

(-2  $\mu$ A). The  $\rho$  and  $\Lambda$  values were calculated as 5.3 and -9600, respectively. This phenomenon is consistent with that we observed with negative overpotential and indicates that the “pumping” of O<sup>2-</sup> from the catalyst can be favorable to the toluene deep oxidation over the Ag catalyst.

From the above results, the conclusion can be drawn that wet impregnation is an effective method for the preparation of Ag film used for EPOC. Taking into account the simple manipulation and cost-effectiveness of this method, we think it may be a feasible way for a practical application of the Ag film catalyst.

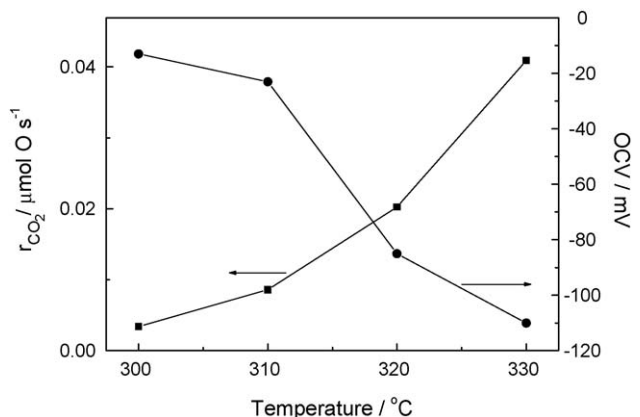
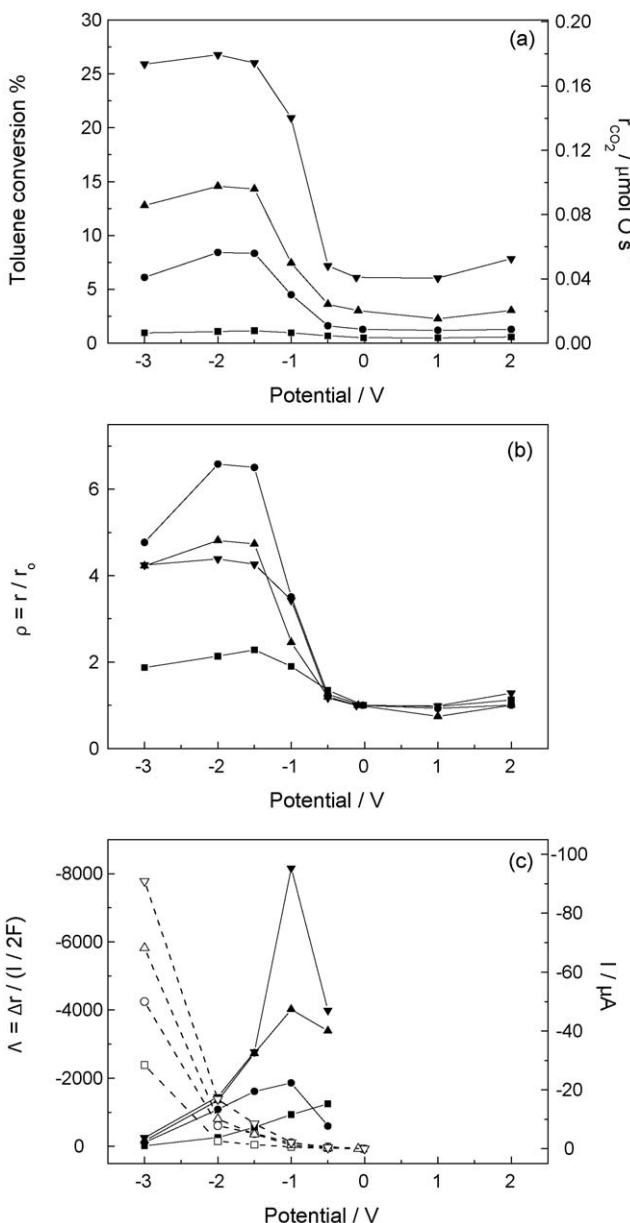


Fig. 4. Open circuit activity of Ag film catalyst (thickness: 1.8  $\mu$ m) deposited on YSZ pellet (■) and the OCV between the work electrode and counter electrode (●) as a function of reaction temperature. Reaction condition: 1% O<sub>2</sub>, 500 ppm toluene, He balance; total flow rate, 100 mL min<sup>-1</sup>.

### 3.2.2. Effect of temperature on the activity of Ag catalyst/electrode submitted to different potentials

Subsequently, we investigated the effect of the reaction temperature on the activity of Ag film catalyst within the temperature range between 300 and 330 °C suggested by Stoukides and Vayenas previous papers [33,38,39]. From Fig. 4, we can see that the activity of Ag film catalyst in the absence of external overpotential increases with the reaction temperature as one would have expected. At the same time, the OCV becomes more and more negative, indicating that Ag surface is free of oxygen (reduced state) [40] or the oxygen adsorption is much weakened. This result may be comprehended by the self-reduction of Ag or AgO decomposition at higher temperature.



**Fig. 5.** Steady state electro-promoted activity of Ag film catalyst (thickness: 1.8  $\mu\text{m}$ ) deposited on YSZ pellet (a), rate enhancement (b), Faradaic efficiency (filled symbol and solid line) and stabilize current (empty symbol and dot line) (c) as a function of applied potential. Reaction condition: 1%  $O_2$ , 500 ppm toluene, He balance; total flow rate, 100  $\text{mL min}^{-1}$ , at 300 °C (■, □); 310 °C (●, ○); 320 °C (▲, △); 330 °C (▽, ▾).

Fig. 5a shows the yields of  $CO_2$  after stabilization at different potentials by potentiostatic operation. From the shape of these curves, we can see that the promotional effect on the Ag catalyst is very significant under the negative overpotential whatever the temperature. Conversely, no activity change of Ag catalyst is observed under positive overpotential. According to the rules of EPOC established by Vayenas et al. [15,41], the catalytic combustion of toluene over Ag film catalyst follows an electrophilic NEMCA behaviour, which can be observed when the electron donor reactant is more strongly adsorbed on the catalyst surface than the electron acceptor reactant. These results can be explained by the fact that toluene is a non-saturated hydrocarbon and has  $\pi$ -electrons in its structure, which make it strongly adsorbed on the surface of Ag as an electron-donor therefore hindering the adsorption of  $O_2$  (an electron-acceptor). The application of a negative potential or current leads to the migration (by electrochemical pumping) of  $O^{2-}$  from the surface of Ag catalyst, thus changes the work function and favors the adsorption of oxygen.

It is very interesting that, in the work of Vayenas et al. over  $RuO_2$  catalyst film deposited on YSZ, a rate enhancement was observed for both anodic and cathodic polarizations (inverted volcano behaviour), with a stronger electrophobic component due to the stronger chemisorption of oxygen on the catalyst surface. This can be understood because (a)  $RuO_2$  is a stable oxide [16], which makes it difficult to form strong chemisorption with toluene by accepting  $\pi$ -electrons (b) the reaction temperature used (450 °C) was quite higher than the one used in the present study. It is well known that high temperature favors the inverted volcano behaviour when both the electron donor and the electron acceptor reactants are weakly adsorbed at the catalyst surface.

Furthermore, it is noticed from Fig. 5b that while increasing the negative potential, the activity of Ag catalyst increased initially, reached a plateau, then decreased more or less according to the temperature used. Such a volcano shape relationship was also observed when we plotted the Faradaic efficiency against the applied overpotential (Fig. 5c). These results can be understood by the competition between the removal and adsorption of the oxygen on the surface of Ag catalyst. Initially and under low negative overpotential, the current is low, the removal of oxygen ions can change the work function and facilitate adsorption of oxygen. As a result, the reaction is accelerated, the yield of  $CO_2$  and Faradaic efficiency increased. With the coverage of catalyst surface by oxygen, the further adsorption of  $O_2$  will become more and more difficult, which leads to the decrease of Faradaic efficiency at the beginning. There is an optimal oxygen coverage of the catalyst

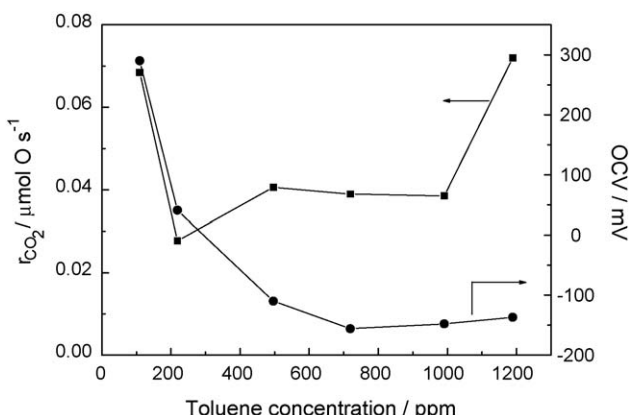


**Fig. 6.** Open circuit activity of Ag film catalyst (thickness: 1.8  $\mu\text{m}$ ) deposited on YSZ pellet (■) and the OCV between the working electrode and counter electrode (●) as a function of toluene concentration. Reaction condition: 1%  $O_2$ , He balance; total flow rate, 100  $\text{mL min}^{-1}$  at 330 °C.

surface. After the optimal coverage of catalyst surface by oxygen is reached, the excess current is only used to maintain the flow of  $O_2^-$  ions from one side of YSZ to other side, thus makes Faradaic efficiency lower and lower. Further negative potential application leads to a surface predominantly covered by oxygen, thus toluene adsorption is hindered. As a result, the activity of the catalyst decreases.

Finally, after comparing the activity and Faradaic efficiency of the Ag catalyst at different reaction temperatures, it was found that the NEMCA effect over the Ag film catalyst was relatively more significant at higher temperature. This can be found by observing variations of OCV: in this reaction, the toluene is electron donor, the oxygen is electron acceptor. With the increasing of the reaction

temperature, the Ag–O bond is weakened, i.e. the surface of Ag catalyst is more predominantly covered with toluene. As the result, after application of negative over potential (enhancing the electron acceptor adsorption), the promotion is more significant at higher temperature. However, if we consider the rate enhancement, the highest one is observed at 310 °C. For practical application purpose, we should keep the reaction temperature as low as possible (the aim of this work). Additionally, from a fundamental point of view, we have to make sure that the reaction is operated under chemical control then at quite low conversion. Taking into consideration the above, the reaction temperature was fixed at 330 °C for further experiments.

### 3.2.3. Effect of toluene concentration on the catalytic activity of Ag catalyst under different potentials

The concentration of VOCs in streams to be treated is likely to vary continuously along the time. Therefore, in this work, we also explored the effect of toluene concentration on the EPOC performance of the Ag film catalyst at 330 °C. To allow a comparison of the results, the concentration of oxygen and total flow rate of reactants were kept at 1% and 100 mL min<sup>-1</sup>, respectively.

As shown in Fig. 6, under OCV condition, when the toluene concentration increased from 100 ppm (oxygen is in much excess, more than ten times the stoichiometric value) to 200 ppm, the rate of  $CO_2$  formation decreased, and the OCV between working electrode and reference electrode decreased as well. While, with the increase of toluene concentration from 200 to 1000 ppm (near-stoichiometric condition), the rate of  $CO_2$  formation stabilized. This can be explained by the competitive adsorption of toluene and oxygen over Ag catalyst, i.e. with the increasing of toluene concentration to more than 200 ppm, the Ag catalyst surface was covered by toluene, the oxygen adsorption was restrained. As a result, the oxidation of toluene was hindered. Further increase of toluene to 1200 ppm led to a higher  $CO_2$  formation rate.

With the application of overpotential, the promotion effects under the various toluene concentrations are also different (Fig. 7). At very low toluene concentration such as 100 ppm (oxygen large excess), the application of either negative or positive overpotential has no significant effect on the  $CO_2$  yield over the Ag catalyst. This can be rationalized by the high OCV (+290 mV), which means the surface of Ag catalyst was dominantly covered by oxygen, and consequently the “pumping” of oxygen species has no effect on the activity of catalyst. After increasing the toluene concentration to 200 ppm, the promotion effect of the overpotential became very

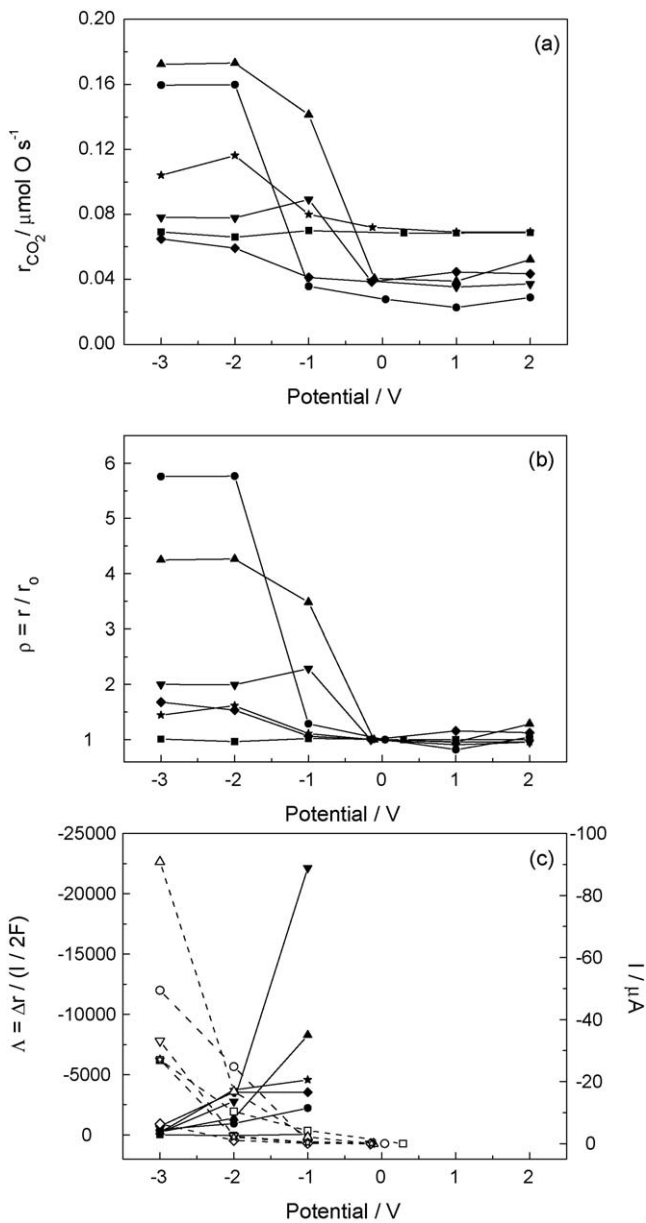


**Fig. 7.** Steady state electro-promoted activity of Ag film catalyst (thickness: 1.8  $\mu$ m) deposited on YSZ pellet (a), rate enhancement (b), Faradaic efficiency (filled symbol and solid line) and stabilize current (empty symbol and dot line) (c) as a function of applied potential. Reaction condition: 1%  $O_2$ , He balance; total flow rate, 100 mL min<sup>-1</sup> at 330 °C. Toluene concentration: 100 ppm (■, □); 200 ppm (●, ○); 500 ppm (▲, △); 700 ppm (▼, ▽); 1000 ppm (◆, ◇); 1200 ppm (★, ☆).

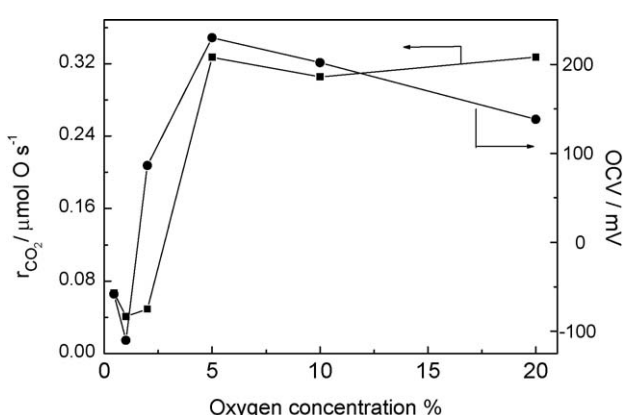


**Fig. 8.** Open circuit activity of Ag film catalyst (thickness: 1.8  $\mu$ m) deposited on YSZ pellet (■) and the OCV between the work electrode and counter electrode (●) as a function of oxygen concentration. Reaction condition: 500 ppm toluene, He balance; total flow rate, 100 mL min<sup>-1</sup> at 330 °C.

evident, as shown by the values of rate enhancement and Faradaic efficiency. Then, with the increasing of toluene concentration from 200 to 700 ppm,  $\Lambda$  continuously increased, while  $\rho$  decreased. This can be rationalized by the decrease of current (less surface oxygen species due to competitive adsorption). Further increase of toluene concentration up to stoichiometric value or toluene rich condition led to the decrease of both  $\rho$  and  $\Lambda$ , which may be interpreted considering the prevailing occupancy by toluene of the active sites at the catalyst surface. Thereby, the impact of oxygen “pumping” upon the catalytic activity was weakened.

### 3.2.4. Effect of oxygen concentration on the catalytic activity of Ag catalyst under different potentials

Analogously to toluene concentration, we also studied the influence of oxygen concentration on the activity of the Ag film

catalyst under different overpotential at fixed toluene concentration (500 ppm), total flow rate ( $100 \text{ mL min}^{-1}$ ) and reaction temperature ( $330^\circ\text{C}$ ).

From the results under OCV conditions (Fig. 8), there is a slight decrease in  $\text{CO}_2$  formation rate and OCV when oxygen concentration switched from 0.45% (stoichiometry) to 1% (oxygen excess), this is similar to what we observed under high toluene concentration. Moreover, it is very interesting that we may observe an abrupt increase of  $\text{CO}_2$  yield accompanied by a leap of OCV when oxygen concentration is above 2%. This phenomenon is similar to what we observed at very low toluene concentration and can be explained by a surface dominantly covered by oxygen.

After applying the negative overpotential (Fig. 9), we found that activity and rate enhancement of Ag catalyst both increased

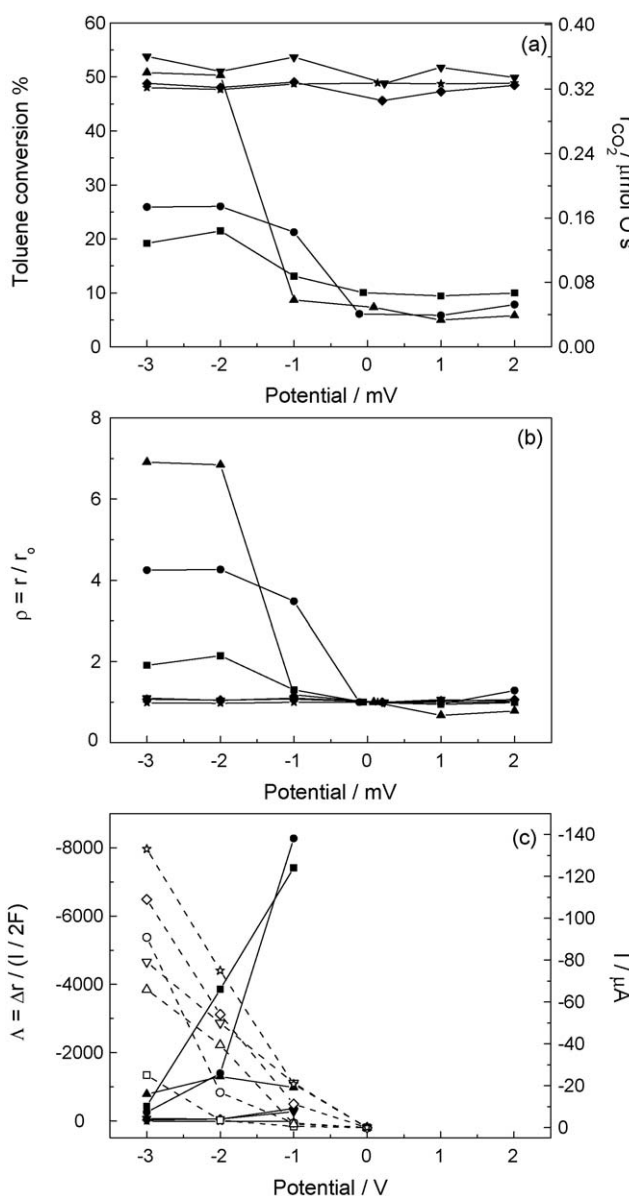


**Fig. 9.** Steady state electro-promoted activity of Ag film catalyst (thickness:  $1.8 \mu\text{m}$ ) deposited on YSZ pellet (a), rate enhancement (b), Faradaic efficiency (filled symbol and solid line) and stabilize current (empty symbol and dot line) (c) as a function of applied potential. Reaction condition: 500 ppm toluene, He balance; total flow rate,  $100 \text{ mL min}^{-1}$  at  $330^\circ\text{C}$ . Oxygen concentration: 0.45% (■, □); 1% (●, ○); 2% (▲, △); 5% (▼, ▽); 10% (◆, ◇); 20% (★, ☆).

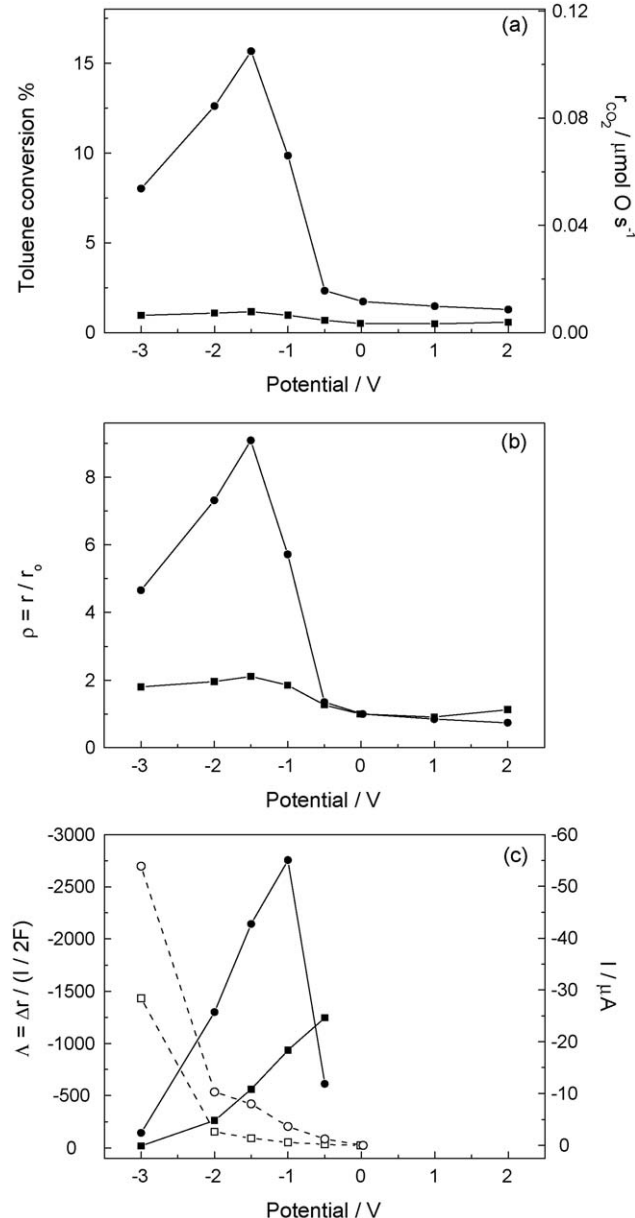


**Fig. 10.** Steady state electro-promoted activity of Ag film catalyst deposited on YSZ pellet (a), rate enhancement (b), Faradaic efficiency (filled symbol and solid line) and stabilize current (empty symbol and dot line) (c) as a function of applied potential. Reaction condition: 1%  $\text{O}_2$ , 500 ppm toluene, He balance; total flow rate,  $100 \text{ mL min}^{-1}$  at  $300^\circ\text{C}$ . Ag film thickness:  $1.8 \mu\text{m}$  (■, □);  $3.9 \mu\text{m}$  (●, ○).

when oxygen concentration increased from 0.45 to 2% while a concomitant decrease of the Faradaic efficiency is observed. This can be explained by the increasing of current and oxygen coverage. When oxygen concentration is higher than 2%, no effect can be observed. Such a result is consistent with results obtained under the very low toluene concentration and means that the Ag film catalyst can only be used in the EPOC for total oxidation of toluene at low oxygen conditions.

### 3.2.5. Effect of Ag film thickness on the catalytic activity of Ag catalyst under different potentials

From previous studies [42–44], it is known that the thickness of catalyst film may also play an important role in the EPOC phenomenon. Therefore, it seemed interesting to investigate the EPOC of toluene combustion over the Ag films of different thicknesses (1.8 and 3.9 µm, respectively) under the same reaction conditions: 1% O<sub>2</sub>, 500 ppm, He balance, at the flow rate of 100 mL min<sup>-1</sup> and 300 °C. Fig. 10 illustrates the CO<sub>2</sub> yield over the Ag film catalyst with different thickness as the function of applied potential. It is obvious that the activity of Ag film increased with the thickness, i.e. with the number of surface sites available, as particle size remains quite unchanged.

Upon the application of negative potential, the promotion and NEMCA effect are more significant for the thicker Ag film. Over the thicker Ag film, particularly rate enhancement (Fig. 10b) but also Faradaic efficiency (Fig. 10c) are obviously higher than those recorded on thinner one under the same reaction conditions. This result is in disagreement with previous NEMCA studies where  $\Lambda$  increases with decreasing catalysts film thickness [45]. From the result of XRD, the effect of catalyst particle size on NEMCA effect as sometimes suggested in the literature [25,46] can be ruled out. The most likely reason maybe a greater number of active centers, which no longer limit the overall reaction rate and then oxygen adsorption modification on these sites is more efficient for EPOC. Another possibility could have been that there are more tpb between YSZ, porous Ag layer and reactants over the thicker layer sample, which leads to enhanced electrochemical promotion. But this is not much supported by the SEM observation. Nevertheless, this shows that quite thick porous layers are necessary to achieve good performance in such a system.

## 4. Conclusions

A significant NEMCA effect was achieved over the Ag catalyst deposited onto YSZ by impregnation with AgNO<sub>3</sub> aqueous solution followed by H<sub>2</sub> reduction. After applying negative external potential or current, prominent rate enhancement and high Faradaic efficiency up to 9600 can be reached, this Faradaic efficiency is comparable to what we previously reported for a paste-made Ag catalyst. Taking into account the simple manipulation and cost-efficiency of the wet impregnation technique, we think it may be a feasible way for Ag EPOC catalyst used for the very important application of the total oxidation of an aromatic VOC as toluene and surely other environmentally important reactions.

From the investigation of different parameters on the EPOC performance of the Ag film catalyst, it was found that the NEMCA effect over the Ag film catalyst is favored by both reaction temperature and Ag film thickness. While, the rate enhancement decreased with toluene concentration but increased with oxygen concentration then vanished when oxygen concentration is higher than 2%. In contrast, the Faradaic efficiency maximized when toluene concentration is about 700 ppm, but decreased with oxygen concentration. This can be explained by the competitive adsorption of toluene and oxygen over the surface of Ag catalyst.

## Acknowledgements

The European Commission is gratefully acknowledged for Marie Curie Incoming International Fellowships (IIF) to support Dr. Ning Li's research work in France. This work was partially funded by the French "Ministère Délégué à la Recherche" in the framework of the "Action Concertée Incitative Energie, Conception Durable", grant No. ECD 048, 2004. The Authors are also pleased to thank Dr. Philippe Vernoux (IRCELYON) for his great help and Dr. Antoinette Boréave (IRCELYON) for technical assistance and fruitful discussion. Mrs Laurence Burel (IRCELYON) is also warmly acknowledged for performing SEM characterization.

## References

- [1] J.J. Spivey, Ind. Eng. Chem. Res. 26 (1987) 2165.
- [2] J. Carpentier, J.F. Lamonier, S. Siffert, E.A. Zhilinskaya, A. Aboukaïs, Appl. Catal. A: Gen. 234 (2002) 91.
- [3] M.-F. Luo, M. He, Y.-L. Xie, P. Fang, L.-Y. Jin, Appl. Catal. B: Environ. 69 (2006) 213.
- [4] R. Spinicci, M. Faticanti, P. Marini, S. De Rossi, P. Porta, J. Mol. Catal. A 197 (2003) 147.
- [5] M. Alifanti, M. Florea, V. Cortes-Corberan, U. Endruschat, B. Delmon, V.I. Pârvulescu, Catal. Today 112 (2006) 169.
- [6] M. Alifanti, M. Florea, V.I. Pârvulescu, Appl. Catal. B: Environ. 70 (2007) 400.
- [7] M. Stoukides, C.G. Vayenas, J. Catal. 70 (1981) 137.
- [8] C.G. Vayenas, S. Bebelis, S. Ladas, Nature (London) 343 (1990) 625.
- [9] P. Vernoux, F. Gaillard, C. Lopez, E. Siebert, J. Catal. 217 (2003) 203.
- [10] X. Li, F. Gaillard, P. Vernoux, Ionics 11 (2005) 103.
- [11] F. Gaillard, X. Li, M. Uray, P. Vernoux, Catal. Lett. 96 (2004) 177.
- [12] P. Vernoux, F. Gaillard, C. Lopez, E. Siebert, Solid State Ionics 175 (2004) 609.
- [13] A.D. Frantzis, S. Bebelis, C.G. Vayenas, Solid State Ionics 136–137 (2000) 863.
- [14] P. Beatrice, C. Pliangos, W.L. Worrell, C.G. Vayenas, Solid State Ionics 136–137 (2000) 833.
- [15] C.G. Vayenas, S. Brosda, C. Pliangos, J. Catal. 203 (2001) 329.
- [16] I. Constantinou, I. Bolzonella, C. Pliangos, Ch. Comninellis, C.G. Vayenas, Catal. Lett. 100 (2005) 125.
- [17] R.M. Lambert, A. Palermo, F.J. Williams, M.S. Tikhov, Solid State Ionics 136 (2000) 677.
- [18] C.A. Cavalca, G.L. Haller, J. Catal. 177 (2) (1998) 389.
- [19] G. Foti, O. Lavanchy, C. Comninellis, J. Appl. Electrochem. 30 (2000) 1223.
- [20] D. Poulidi, A. Thurnfield, I.S. Metcalfe, Top. Catal. 44 (2007) 435.
- [21] N. Li, F. Gaillard, A. Boréave, Catal. Commun. 9 (2008) 1439.
- [22] C. Kokkofitis, G. Karagiannakis, S. Zisekas, M. Stoukides, J. Catal. 234 (2005) 476.
- [23] C. Kokkofitis, G. Karagiannakis, M. Stoukides, Top. Catal. 44 (2007) 361.
- [24] M.F. Al-Kuhaili, J. Phys. D: Appl. Phys. 40 (2007) 2847.
- [25] F. Dorado, A. de Lucas-Consuegra, P. Vernoux, J.L. Valverde, Appl. Catal. B: Environ. 73 (2007) 42.
- [26] F. Dorado, A. de Lucas-Consuegra, C. Jiménez, J.L. Valverde, Appl. Catal. A: Gen. 321 (2007) 86.
- [27] A. de Lucas-Consuegra, F. Dorado, C. Jiménez-Borja, J.L. Valverde, Appl. Catal. B: Environ. 78 (2007) 222.
- [28] A. de Lucas-Consuegra, F. Dorado, J.L. Valverde, R. Karoum, P. Vernoux, J. Catal. 251 (2007) 474.
- [29] A. de Lucas-Consuegra, F. Dorado, J.L. Valverde, R. Karoum, P. Vernoux, Catal. Commun. 9 (2008) 17.
- [30] P. Vernoux, F. Gaillard, L. Bultel, E. Siebert, M. Primet, J. Catal. 208 (2002) 412.
- [31] I. Constantinou, D. Archontis, S. Brosda, M. Lepage, Y. Sakamoto, C.G. Vayenas, J. Catal. 251 (2007) 400.
- [32] R.C. Weast, Handbook of Chemistry and Physics, 59th ed., CRC Press, Palm Beach, USA, B-162, 1979.
- [33] C.G. Vayenas, S. Bebelis, C. Pliangos, S. Brosda, D. Tsiplikides, Electrochemical Activation of Catalysis, Kluwer Academic/Plenum, New York, 2001.
- [34] S. Balomenou, D. Tsiplikides, A. Katsounis, S. Thiemann-Handler, B. Cramer, G. Foti, Ch. Comninellis, G.C. Vayenas, Appl. Catal. B: Environ. 52 (2004) 181.
- [35] D. Tsiplikides, S. Balomenou, A. Katsounis, D. Archontis, C. Koutsodontis, C.G. Vayenas, Catal. Today 100 (2005) 133.
- [36] C.G. Vayenas, S. Bebelis, I.V. Yentekakis, H.-G. Lintz, Catal. Today 11 (1992) 303.
- [37] J.K. Hong, I.-H. Oh, S.-A. Hong, W.Y. Lee, J. Catal. 163 (1996) 95.
- [38] M. Stoukides, C.G. Vayenas, J. Catal. 64 (1980) 18.
- [39] M. Stoukides, C.G. Vayenas, J. Catal. 69 (1981) 18.
- [40] L. Bultel, C. Roux, E. Siebert, P. Vernoux, F. Gaillard, Solid State Ionics 166 (2004) 183.
- [41] S. Brosda, C.G. Vayenas, J. Wei, Appl. Catal. B: Environ. 68 (2006) 109.
- [42] C. Koutsodontis, A. Katsounis, J.C. Figueroa, C. Cavalca, C.J. Pereira, C.G. Vayenas, Top. Catal. 38 (2006) 157.
- [43] C. Koutsodontis, A. Katsounis, J.C. Figueroa, C. Cavalca, C. Pereira, C.G. Vayenas, Top. Catal. 39 (2006) 97.
- [44] A. Billard, P. Vernoux, Top. Catal. 44 (2007) 369.
- [45] C. Koutsodontis, A. Katsounis, J.C. Figueroa, C. Cavalca, C.J. Pereira, C.G. Vayenas, Top. Catal. 38 (2006) 157.
- [46] P. Vernoux, F. Gaillard, R. Karoum, A. Billard, Appl. Catal. B: Environ. 73 (2007) 73.